EFFECT OF THE PRESENCE OF INTERSTITIAL BRINE ON GAS-OIL CAPILLARY PRESSURE

F. Pairoys, D. Simons, K. Bohn, M. Alexander, V. Odu, R. DeLeon, J. Ramos
Schlumberger Reservoir Laboratories, Houston, Texas, 77041, United States

This paper was prepared for presentation at the International Symposium of the Society of Core Analysts held in Newfoundland and Labrador, Canada, 16-20 August, 2015

ABSTRACT

Gas-oil centrifuge capillary pressure experiments were performed on two outcrop samples in the presence and absence of a third immobile phase in order to highlight effects on final recovery.

Two core plugs with different porosity and permeability properties were respectively drilled from an Indiana limestone block and Berea sandstone block. They were solvent cleaned and measured for routine core analysis before starting the SCAL program. Two centrifuge capillary pressure experiments were run on the samples at different saturation conditions. Both samples were first saturated with brine and displaced by oil up to irreducible brine saturation using centrifuge (primary drainage). Gas-oil gravity drainage was then performed using multistep centrifuge method for capillary pressure measurement. The samples were then cleaned, measured again for basic properties, and saturated with oil. The second experiment was a new gas-oil multistep centrifuge drainage using same capillary pressure steps than in the first test, but directly performed on the samples initially saturated with oil.

The objective was to highlight the effect of the interstitial brine on the capillary pressure curves and on the oil recovery. It is finally shown that the use of only two phase capillary pressure may result in an invalid capillary pressure relationship between the two mobile fluids in the presence of a third. The Hassler-Brunner method for the determination of the local capillary pressure curves in presence and absence of a third phase is discussed. The study also confirms the necessity of using the Forbes method to avoid inaccurate data results.

INTRODUCTION

Almost all reservoirs contain three fluid phases within their pore network, respectively water, oil and gas. Water and oil are immiscible together, whereas gas can be miscible with oil or/and can be dissolved in the aqueous phase according to the reservoir conditions and fluid properties. Assuming that miscibility and dissolution are not involved, the three phases may be mobile or static according to their saturations; in a three phase system, there is at least one mobile phase. The capillary pressure P_c is an important parameter for the reservoir engineers who are using this petrophysical input in their numerical simulations, in addition to the relative permeability K_r, to anticipate the

reservoir behavior. Capillary pressure P_c is a two-phase phenomenon resulting from a discontinuity in pressure across the interface between two immiscible fluids. Capillary pressure is affected by a multitude of parameters; fluid properties, saturation, saturation history [1], pore size, pore shape, pore distribution, tortuosity, wettability [4]. It is evident that oil recovery in a reservoir is affected by the capillary pressure P_c since trapping mechanisms depends on the listed parameters.

Gravity drainage is the drainage process of gas displacing oil in a reservoir or sample. In certain cases, it is an efficient recovery mechanism which can result in very low residual oil saturation compared to waterflooding displacements [2]. Three phase capillary pressure test as described by Kantzas *et al.* [3] with three mobile phases is not considered in this study; two phase -gas/oil- capillary pressure experiments in presence or absence of a third immobile phase -brine- are investigated. Hassler *et al.* [4] and other others such as Kyte *et al.* [5] or Hagoort [6] concluded that the gravity drainage could be considered as two phase flow displacement at low water irreducible saturation. There is a lack in experimental investigation of the effect of connate water on the final oil recovery during gravity drainage. Dumore [7] showed that the presence of connate water during gravity drainage test in permeable medium leads to very low residual saturations due to film flow [8]. Hagoort [6] observed a decrease in residual oil saturation with an increase of water saturation due to more streamlined flow channels. One study from Carlson [9] showed that the presence of irreducible water had no effect on the residual oil saturation. Earlier, a same observation was made by Tiffin and Yellig [10].

The purpose of this paper is to compare gas-oil capillary pressure in presence or absence of connate water during a multistep centrifuge experiments. The centrifuge tests were performed at ambient conditions and immiscible conditions. Because capillary pressure is, *inter alia*, affected by pore size, two different rock types were tested to compare the effect of irreducible water on the final oil recovery during drainage cycle. The Hassler-Brunner method [4] to calculate the local capillary pressure at the inlet of the core samples is also discussed in this paper. The core analysis software CYDAR was used for data processing.

BACKGROUND

In centrifuge gravity drainage experiments, the fluid flow is controlled by the density difference between fluids. The local velocity u for each fluid is given by the generalized Darcy's law:

$$u = -\frac{KK_r}{\mu}\left(\frac{\partial P}{\partial x} - \rho\omega^2 r\right) \quad (1)$$

With K the absolute permeability in m^2, K_r the relative permeability, μ the fluid viscosity in Pa.s, P the fluid pressure in Pa, ρ the fluid density in Kg/m^3, ω the rotational speed in rad/s and r the distance between the position on the rock sample and the centrifuge axis in m.

The capillary pressure P_{ce} at the inlet of a sample during a centrifuge experiment can be expressed as follows:

$$P_{ce} = \frac{1}{2}\Delta\rho\omega^2\left(r_2^2 - r_1^2\right) \quad (2)$$

With P_{ce} the inlet capillary pressure in Pa, $\Delta\rho$ the density contrast between the two fluids in Kg/m^3, r_2 the distance between the outlet of the sample and the centrifuge axis in m, and r_1 the distance between the inlet of the sample and the centrifuge axis in m.
A sketch of rock sample loaded in centrifuge core holder is shown below:

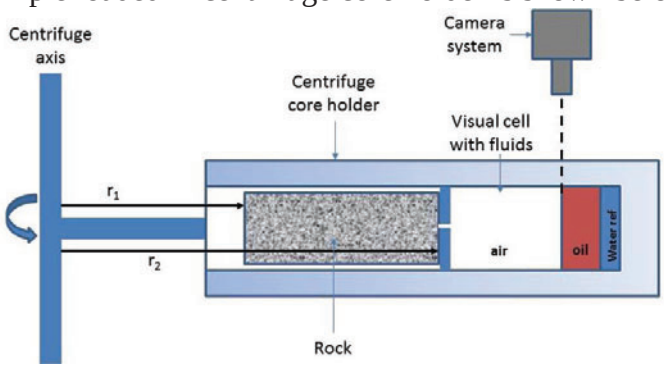

Figure 1: Sketch of core plug loaded in centrifuge core holder

During a multi-speed experiment, when the production of the displaced phase ceases at the end of each rotational speed, the average saturation <*S*> can be calculated from the effluent production. <*S*> is linked to the local inlet capillary pressure P_{ce} at equilibrium by the following Hassler and Brunner equation:

$$\langle S(P_{ce})\rangle = \frac{1}{r_2 - r_1}\int_{r_1}^{r_2} S(P_{ce})dr \quad (3)$$

The Hassler-Brunner method [4] is commonly used in the industry to approximate the local saturation at the capillary pressure P_{ce} using the following equation:

$$S(P_{ce}) = \frac{d}{dP_{ce}}\left[P_{ce} < S(P_{ce})>\right] \quad (4)$$

The differentiation of this equation was performed by differentiating a modified hyperbolic function which best fits the product P_{ce}<$S(P_{ce})$>. The Forbes method [11] after smoothing the data [13] was used when the Hassler-Brunner method did not give satisfying local capillary pressure curve.

The Hassler-Brunner method is valid for short cores spinning far enough from the centrifuge axis to assume that the variation of the centrifugal field is negligible; in this study, the ratio r_1/r_2 in Figure 1 was found to be equal to 0.6. The maximum Bond number N_b obtained at the highest speed was less than 10^{-4}.

ROCKS, FLUIDS AND EXPERIMENTAL SETUP

Two rock types were tested respectively Berea sandstone and Indiana limestone. Berea sandstone is unimodal in pore and pore throat sizes whereas Indiana limestone is bimodal. It is confirmed by mercury injection capillary pressure (MICP) and NMR T_2 distributions obtained respectively from two rock chips and two 100% brine saturated core samples cut from each block (Figure 2):

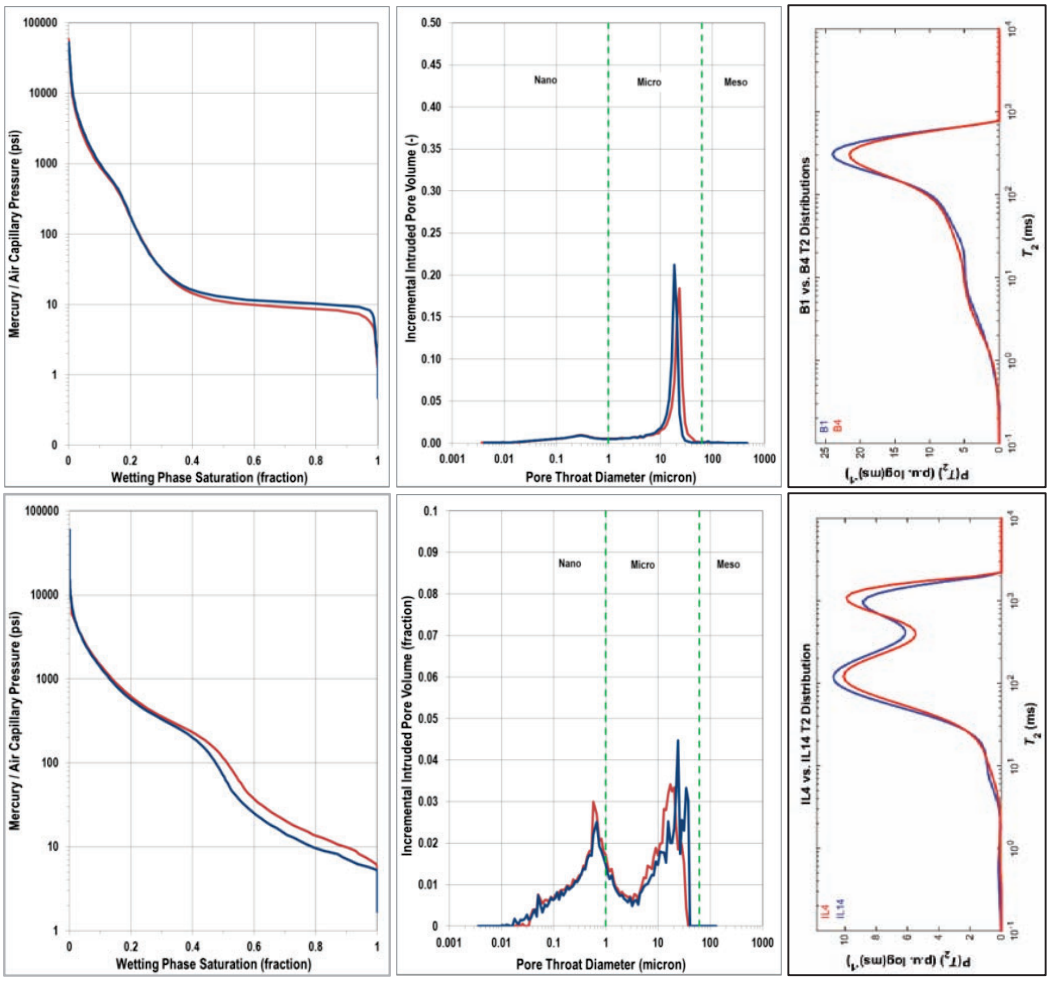

Figure 2: Capillary pressure (left), pore throat size distribution (middle) and NMR T_2 distribution (right)

Figure 2 shows that the two rock types have different signatures as expected and also shows that measurements on twin plugs obtained from the same block are almost identical. The two samples tested in this study came from the same blocks as the samples tested for MICP and T_2 NMR from Figure 2. There is a clear correlation between the NMR pore size distribution and the MICP pore throat distribution for each rock type. Both MICP and NMR highlight respectively the unimodal pore structure of the Berea sandstone and bimodal pore structure of the Indiana limestone. Additional rock information obtained from the same Berea sandstone and Indiana limestone blocks can be

found in Pairoys *et al.* [14].

Several core plugs were obtained from the Berea sandstone Indiana limestone blocks, but only data results of sample B2 (Berea sandstone) and sample IL20 (Indiana limestone) are reported. After having Soxhlet cleaned the samples, routine core analysis was performed on the samples. Data results are listed in Table 1:

Table 1: Dry core plug properties

Sample Id	Type	ρ_g (g/cc)	ϕ (%)	PV (cc)	K_g (mD)	K_{kl} (mD)
B2	Berea sandstone	2.65	25.23	10.473	735.7	727.8
IL20	Indiana limestone	2.69	15.43	6.772	31.8	30.4

Fluid properties (brine, oil and air) at ambient temperature and atmospheric pressure are reported in Table 2:

Table 2: Fluid properties

Fluid	Salinity (Kppm NaCl)	Density ρ (g/cc)	Viscosity μ (cp)
Brine	200	1.130	1.345
Isopar-L	-	0.762	2.049
Air	-	0.001	0.018

The capillary pressure experiments were run with an Ultra Rock Centrifuge from Beckman allowing monitoring fluid production using a camera system. The two samples were first saturated with Isopar-L before being loaded in drainage centrifuge cells and tested for multistep capillary pressure P_c. Ten P_c steps were applied, from 0 to 84 psi.
At the end of the drainage cycle, the samples were Soxhlet cleaned using Toluene and Methanol, dried, and re-measured for gas permeability and porosity. Because the rock properties did not change after the first P_c test and cleaning, they were used again for the second P_c test in presence of connate water. The two cleaned samples were then saturated with brine, loaded in drainage cells for brine-oil primary drainage up to irreducible water saturation S_{wi} using one single maximum step (8000 rpm – around 100 psi for all samples). Then, they were tested in the same drainage core holders for gas-oil displacement. They were spun at the exact same capillary pressure steps than those applied during the first test with samples initially saturated with oil.

EXPERIMENTAL RESULTS

Centrifuge gas-oil capillary pressure experiments were run on the two samples, IL20 and B2, initially 100% saturated with oil and later saturated with oil at irreducible water saturation S_{wi}. The main objective is to see if the capillary pressures curves and productions are affected by the presence of irreducible water saturation.

Gas-Oil Drainage at Initial Oil Saturation S_o=100%:
The samples B2 and IL20 were directly tested for gas-oil multistep capillary pressure. Ten capillary pressure steps were applied; they were chosen according to a preliminary designing test on sample IL20 100% oil saturated only (using CYDAR software). The average saturations were fitted with a bi-exponential curve to obtain the average saturation at equilibrium. Figure 3 represents the oil production curves during the centrifuge P_c experiment.

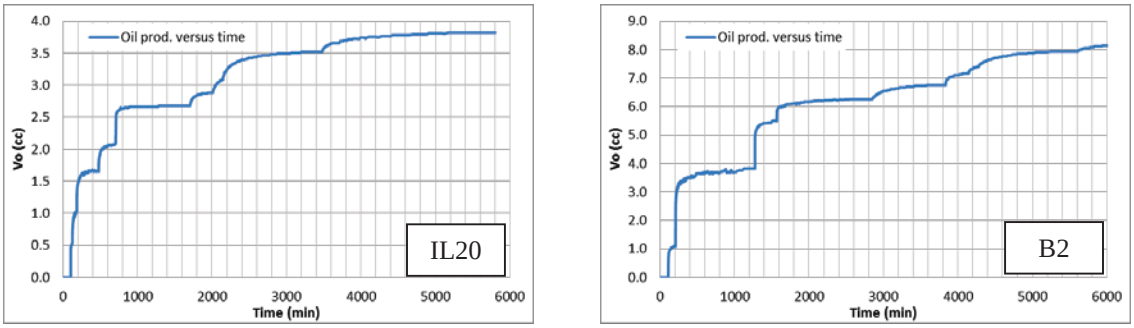

Figure 3: Drainage oil productions (raw data) for samples IL20 (left) and B2 (right)

Sample IL20: A total of 3.82 cc of oil was produced, leading to residual oil saturation S_{or} close to 43.6%. S_{or} was found to be high due to the presence of the oil-filled nanopore population highlighted in Figure 2; at the applied pressure steps, it is not possible to displace the oil in these tiny pores. The production curve also shows that equilibrium was not completely reached at all P_c steps. The oil production was fitted with multistep bi-exponential function to obtain the saturation at equilibrium.

Sample B2: A total of 8.40 cc of oil was produced from sample B2. The residual oil saturation was found to be equal to 19.8%, significantly lower than for the Indiana limestone IL20; these two rocks have different pore size and throat signatures, partially responsible for this difference.

In Figure 4, the capillary pressures P_c versus average oil saturations S_o at equilibrium are plotted for both samples (in blue). Modified hyperbolic functions were used to fit the capillary pressure curves before calculating the local saturations (in red). Local capillary pressure curve is obtained from Hassler and Brunner method in green). As QC technique, the average saturations $<S_o>$ were recalculated (in purple) and compared to the analytical P_c curves (in red) in order to assess the Hassler-Brunner method.

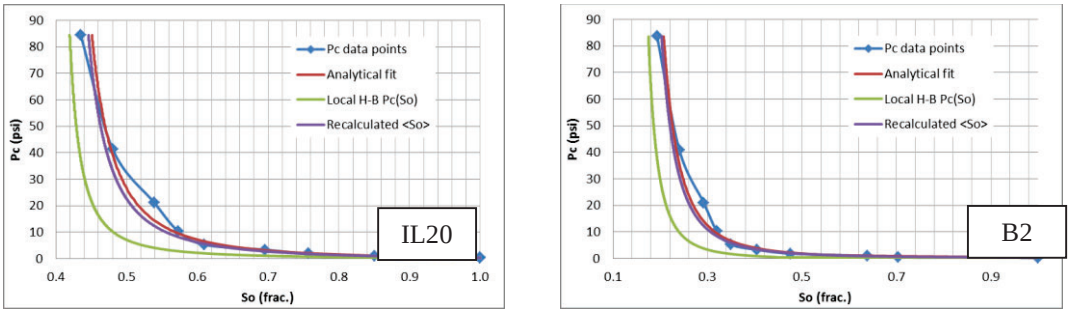

Figure 4: Measured, analytical fit, local Hassler-Brunner and recalculated capillary pressure curves

Figure 4 shows that the Hassler and Brunner method provides more acceptable result for sample B2 than for sample IL20; the recalculated average saturation matches well the analytical fitted curve. The exact same experimental protocol was performed on the same cores but at irreducible saturation S_{wi} as initial condition.

Gas-Oil Drainage at Initial Irreducible Water Saturation S_{wi}:

For the sake of more clarity, an asterisk * was added to the plug number containing irreducible water at initial conditions. At the end of the previous test, samples were Soxhlet cleaned, dried and measured for routine core analysis; porosity and permeability were found were close to the ones reported in Table 1. After brine saturation of sample B2* and IL20*, a primary drainage, oil displacing brine, was performed. They were spun in centrifuge at a single speed of 8,000 rpm, so approximatively 100 psi of oil-brine capillary pressure P_c up to irreducible water saturation S_{wi}. Cores were also flipped to get a more uniform fluid distribution along the samples [15]. The irreducible water saturation S_{wi} for sample IL20* was found to be equal to 36.1% whereas S_{wi} for sample B2* was found to be equal to 16.6%. The presence of nanopores (Figure 2) explains the high S_{wi} value for sample IL20*. The samples were then loaded in the drainage centrifuge cells for air-oil multistep capillary pressure experiment. Tests were run with the same capillary pressure steps than those applied on the samples initially saturated with oil. No brine production was observed during the gas-oil centrifuge P_c experiments.

IL20*

The same increasing capillary pressure steps were applied during the gas-oil drainage displacement of sample IL20*.

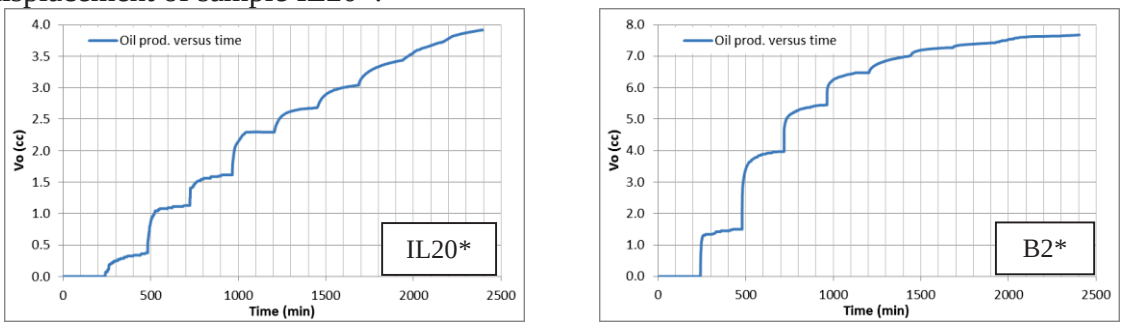

Figure 5: Drainage oil productions (raw data) for sample IL20* (left) and B2* (right)

Figure 5 represents the oil production versus time during the multistep centrifuge experiment with samples initially at S_{wi}. The production curves show that equilibrium was not completely reached at all P_c steps, leading to an overestimation of the residual oil saturation S_{or}. The same fitting process than the one described on the experiment with samples initially saturated with oil was used to obtain the saturation at equilibrium.

Sample IL20*: A total of 3.92 cc of oil was produced, leading to residual oil saturation S_{or} close to 6.1%. The produced volume was found to be almost the same than the one obtained on the same sample initially saturated with oil. It is explained by the bimodal porosity system of this limestone rock. Only oil occupying the micro-pore population highlighted in Figure 2 can be mobilized and produced. The main difference is the final recovery of the original oil in place (OOIP), which is obviously much higher when the water occupied the small pores (nano-pores population for this Indiana limestone rock).

Sample B2*: A total of 7.68 cc of oil was produced from sample B2, leading to 10.1% of residual oil saturation. The oil production was found to be less than the one obtained for the same sample at 100% oil initial condition. The capillary pressure P_c versus average oil saturation S_o at equilibrium is then plotted for both samples (blue curve in Figure 4):

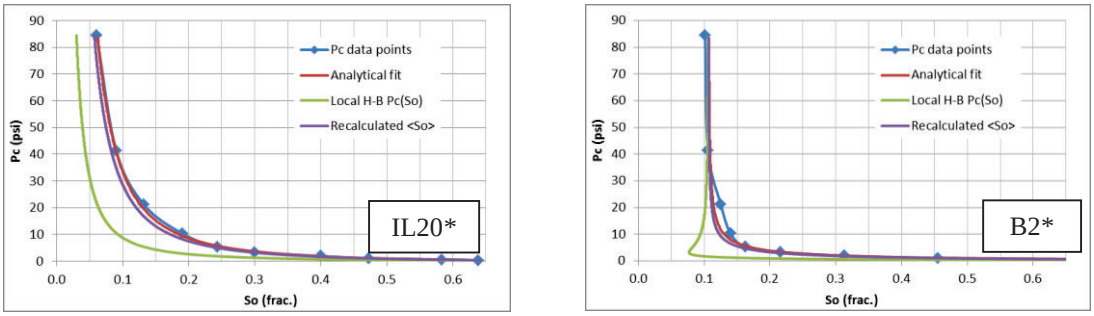

Figure 6: Measured, analytical fit, local H-B and recalculated capillary pressure curves

As observed in Figure 4 for samples initially saturated with oil, the back calculation of average oil saturation $<S_o>$ for sample IL20* does not perfectly fit the analytical curve used for fitting the P_c data points. The non-monotonic local P_c of sample B2* obtained with the Hassler-Brunner method may be explained by the choice of the modified hyperbolic fitting function and the imperfect equilibrium of the P_c data points. Despite of this observation, an acceptable match between analytical data fit P_c (red) and recalculated P_c at average saturation (purple) is obtained for sample B2*.

For the local P_c calculation, whatever the initial conditions (with or without presence of irreducible water saturation), the Hassler and Brunner method seems more appropriate for the sandstone sample B2/B2*; the match between the analytical function used to fit the P_c data points and the recalculated $<S_o>$ function for the Indiana limestone is less good than the match of the same curves for the Berea sandstone. The reason could be the bimodal character of the limestone rock. Because of the non-monotonic Hassler-Brunner local P_c curve of sample B2* shown in Figure 6, the Forbes method with initial splines fit was

tested (Figure 7):

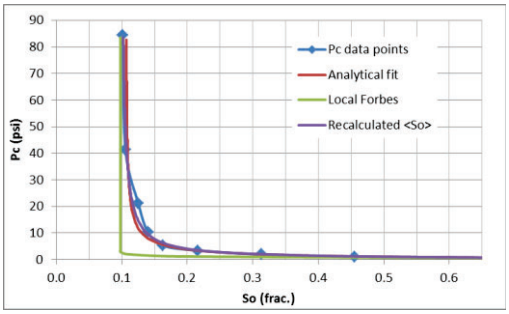

Figure 7: Measured, analytical fit, Forbes-splines and recalculated <.S_o> P_c curves for sample B2*

In addition to the observed monotonic local P_c curve, the match between the analytical and recalculated P_c was improved using Forbes method with splines. All capillary pressure curves P_c were then normalized for saturation (reduced oil saturation S_o* on X axis), plotted on a same graph, and compared (Figure 8).

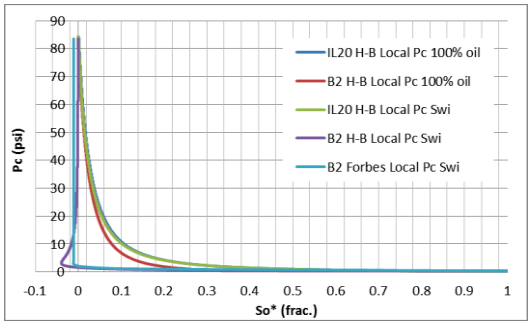

Figure 8: Comparison of local P_c curves for sample IL 20 and B2, S_o=100% versus initial Swi

Figure 8 shows that, whatever presence or absence of irreducible water, the local capillary pressure curves of IL20/IL20* are overlapping. Using two phase capillary pressure centrifuge test without connate water may be representative of the two phase capillary pressure with connate water for this sample. However, for sample B2/B2*, the capillary pressure curves are different. In that case, the use of two phase capillary pressure without connate water may not be representative of the two phase capillary pressure with connate water. One of the reasons may be the change of gas-oil interface curvature in presence of irreducible water.

Additional tests need to be performed to confirm that the Hassler-Brunner outflow condition was not violated due to high Bond number N_b, invalid constant centrifugal field condition (geometry), or presence of irreducible water at the outlet of the samples. NMR or X-ray measurements before and after the gas-oil drainage displacement could help in ensuring that the outlet saturation does not change. The failure of Hassler-Brunner method for obtaining reliable local P_c curve for B2* may also be due to one or combination of the enounced factors, showing the complexity of such experiments.

Recovery Analysis:
Table 3 compares the productions at different initial conditions, with and without irreducible water saturation. For the sake of more clarity, an asterisk * was added to the plug number containing irreducible water at initial conditions.

Table 3: Summary of production according to the initial conditions

Sample Id	*PV* (cc)	S_{wi} (frac.)	S_o (frac.)	V_o prod. (cc)	ORF (%)	S_{or} (frac.)	S_g (frac.)	$K_g(S_{or})$ (mD)
IL20	6.77	0.000	1.000	3.82	56.4	0.436	0.564	32.9
IL20*	6.77	0.361	0.639	3.92	90.5	0.061	0.579	31.8
B2	10.47	0.000	1.000	8.40	80.2	0.198	0.802	747.8
B2*	10.47	0.166	0.834	7.68	87.9	0.101	0.734	727.0

Sample IL20/IL20*:
The presence of irreducible water S_{wi} in IL20* results in very low residual oil saturation S_{or} close to 6.1%. It can be explained by the rock water wettability. First, the small pores are initially saturated with brine; no oil could displace the water in the nanopore zone. Then, water spreads on the pore wall, making easy the oil displacement by gas in the large pores. It also explains the large oil recovery factor ORF of IL20* with almost 90.5% of the original oil in place produced by gas. The gravity drainage in IL20 (no S_{wi}) is much less efficient. The main reason is that oil initially trapped in nanopores (see Figure 2) cannot be mobilized by gas at the applied capillary pressure steps, in addition to the oil wettability of the rock in presence of oil and gas only (no lubrication effect like IL20*). Around 56.4% of oil in place was recovered; this value can be considered low compared to the generally high recovery (>60% from case histories) observed during gravity drainage at secondary conditions (no waterflooding before gas injection in oil reservoirs).

Sample B2/B2*:
The residual oil saturation and recovery factor of sample B2/B2* are less affected by the presence or absence of irreducible water saturation S_{wi} compared to IL20/IL20*. One of the reasons is the unimodal signature of the pore space. The oil recovery factor is higher in presence of connate water. It is also observed that the values at S_{or} of B2 and IL20 are in the same range but slightly higher than the values of S_{wi} of B2* and IL20*; same range because the capillary trapping mechanism is similar for both tests (B2 being oil-wet in presence of gas only and B2* being water-wet in presence of gas and oil) and slightly higher gas/oil S_{or} than brine/oil S_{wi} because of the difference in maximum applied P_c (100 psi for oil displacing brine up to S_{wi} and 85 psi for gas displacing oil up to S_{or}).
Steady-state gas permeability measurements were performed on the samples at the end of the gas-oil drainage to obtain the relative permeability k_g at S_{or}. Results are reported in Table 3 as well. It shows that for sample IL20/IL20*, the presence of a third immobile phase does not change the effective permeability to gas; both values at S_{or} and at S_{or} and S_{wi} are similar. One of the reasons is that, in presence or absence of irreducible water, the

couple IL20/IL20* and the couple B2/B2* have close final gas saturation S_g; whatever liquids (oil or water + oil) are inside the rock, they do not affect the flow of the strongly non-wetting phase such as gas. The effective gas permeabilities are also very close to the absolute gas permeabilities (Table 1). The residual oil and irreducible water do not hamper gas flow because gas is strongly non-wetting the rock compared to liquids. Effective permeability values are even slightly higher than the absolute one; this phenomenon is known as lubrication effect [16].

At the end of the experiment, the samples initially saturated with brine were Dean Stark extracted to validate the irreducible water saturation S_{wi} obtained by material balance during the primary drainage. Irreducible water saturation S_{wi} obtained by material balance during the centrifuge tests and irreducible water saturation obtained by Dean-Stark were found to be very close, ensuring that no connate water was dried or produced during the gas injection. Moreover, to ensure that the samples were not damaged during the centrifuge tests, porosity and absolute gas permeability were measured; no significant rock property changes were observed (Table 4).

Table 4: Dean Stark results and dry rock properties before and after the tests

Sample Id	Material balance S_{wi} (frac.)	Dean Stark S_{wi} (frac.)	Initial ϕ (%)	Final ϕ (%)	Initial K_g (mD)	Final K_g(mD)
B2*	0.166	0.159	25.23	25.40	735.7	728.6
IL20*	0.361	0.355	15.43	15.24	31.8	31.0

CONCLUSION

Two-phase, gas-oil, centrifuge capillary pressure measurements were performed on different rock types in presence or absence of interstitial water. Two different rock types were tested to assess the effect of pore size distribution on final oil recovery. Results of the investigation show that a third brine phase saturation can significantly change the residual oil saturation S_{or} and the oil recovery factor ORF, the shape of the capillary pressure curve and saturation distribution in the cores. It is also shown that the Hassler and Brunner method, used for determining the inlet saturation in centrifuge experiments, can be improved using Forbes method with splines. It is finally concluded that the presence of a third phase can have a significant effect in determining the capillary pressure-saturation relationships between two fluids in a three phase system. Additional work is required for validating the Hassler-Brunner outlet boundary condition using NMR or X-ray spectroscopy.

For oil recovery, the rock saturation history is an important parameter: more oil volume is obtained from samples initially saturated with oil, but higher oil recovery factor ORF is observed in presence of irreducible water. It is also very important to know the pore size/pore throat distributions to get a better understanding of the oil production scenario. The gas floods leads to low residual saturation in swept zones but poor volumetric rock sweep in the bimodal Indiana limestone sample initially saturated with oil.

REFERENCES

1. Brown, R.J.S., Fatt, I., "Capillary Pressure Investigations", *Trans. AIME*, **192**, pp. 67-74, 1951
2. Leverett, M.C., "Capillary Behavior in Porous Solids", *Trans. AIME*, **142**, pp. 152-169, 1941
3. Kantzas, A., Chatzis, I., Dullien, F.A.L., "Enhanced Oil Recovery by Inert Gas Injection", SPE/DOE Paper 17379, 1988
4. Hassler, G.L., Brunner, E., "Measurement of Capillary Pressure in Small Core Samples", *Trans. AIME* 160:114-123, 1945
5. Kyte, J.R., Stanclift, R.J. Jr., Stephan, S.C., Rapoport, L.A., "Mechanism of Water Flooding in the Presence of Free Gas", *Trans. AIME*, **207**, pp. 215-221, 1956
6. Hagoort, J., "Oil Recovery by Gravity Drainage", *SPE Journal*, pp. 139-150, June 1980
7. Dumore JM, Schools RS, "Drainage Capillary Pressure Functions and the Influence of Connate Water", SPE 4096, *SPE Journal*, pp. 437-444, October 1974
8. Nenniger, E. Jr., Storrow, J.A., "Drainage of Packed beds in Gravitational and Centrifugal-Force Fields", *AIChE*, Vol. 4, Issue 3, pp. 305-316, September 1958
9. Carlson, L.O., "Performance of Hawkins Field Unit Under Gas Drive – Pressure Maintenance Operations and Development of EOR Project", SPE/DOE paper 17324, 1988 SPE/DOE Symposium on EOR, Tulsa, Oklahoma, US, 17-20 April 1988
10. Tiffin, D.L., Yellig, W.F., "Effects of Mobile Water on Multiple-Contact Miscible Gas Displacement", *SPE Journal*, pp. 447-455, June 1983
11. Forbes, P., "Simple and Accurate Methods for Converting Centrifuge Data into Drainage and Imbibition Capillary Pressure Curves", Society of Core Analysts, SCA1991-07, 1991
12. Nordtved, J.E., Kolitvelt, K., "Capillary Presure Curves from Centrifuge Data by Use of Spline Functions", *SPERE*, pp. 497-501, November 1991
13. Bauget, F., Gautier, S., Lenormand, R., Samouillet, A., "Gas-Liquid Relative Permeability from One-Step and Multi-Step Centrifuge Experiments", Society of Core Analysts, SCA2012-13, Aberdeen, Scotland, 27-30 August, 2012
14. Pairoys, F., Nadeev, A., Kirkman, K., Poole, G., Bohn, K., Alexander, M., Radwan, N., Abdallah, W., Akbar, M., "Assessment of Sidewall Cores for Routine and Special Core Analyses", Society of Core Analysts, SCA2015-A003, Newfoundland and Labrador, Canada, 16-20 August 2015, Scotland, 27-30 August, 2012
15. Pairoys, F., Al-Zoukani, A., Nicot, B., Valori, A., Ali, F., Zhang, T., Ligneul, P., "Multi-Physics Approach for Aging Assessment of Carbonate Rocks", SPE 149080, Society of Petroleum Engineer, ATSE, Al-Khobar, Saudi Arabia, 15-18 May 2011
16. Berg, S., Cense, A.W., Hofman, J.P., Smits, R.M.N., "Flow in Porous Media with Slip Boundary Condition", Society of Core Analysts, SCA2007-13, Calgary, Canada, 10-12 September 2007